MODELLING OF NON-UNIQUE STATIONARY REGIMES IN CARBON FILTRATION COMBUSTION

Andrey V. BEKKER[1], Iztok LIVK[2] and Eugene V. POLIANCZYK

IPCP RAS, Chernogolovka, Moscow region, 142432 RUSSIA
[2]Parker CRC for Integrated Hydrometallurgy Solutions, CSIRO Minerals, Bentley WA 6982, AUSTRALIA

ABSTRACT

A dynamic mathematical model of co-flow filtration combustion of carbon-containing material in gas flow is presented. Based on this 2-D distributed process model, analysis of process behaviour was facilitated by means of analytical and numerical methods. A fully implicit finite-element approximation of the set of nonlinear partial differential equations was solved iteratively using Newton's method and adaptive mesh strategy. Numerical experiments revealed a new physical phenomenon in terms of the existence of non-unique stationary regimes of filtration combustion of carbon. Upon switching from one regime to another, both the temperature in the combustion front and velocity of propagation of front substantially change, and so does the composition of combustion products. Numerical simulations, carried out using the same process model, showed that non-unique stationary regimes are also possible in other similar processes, such as magnesium carbonate and calcium carbonate roasting.

NOMENCLATURE

c	heat capacity
C	molar ratio of carbon/silica in a solid fuel
D	diffusion coefficient of the gas in the bulk between solid particles
E	activation energy
G_0	total gas flow rate
h	convective heat transfer coefficient
k	pre-exponential factor of the rate constant for a chemical reaction
k_0	pre-exponential factor of the molar rate constant for a chemical reaction
m	pore volume per unit layer volume, or porosity
M	molar mass
$\boldsymbol{n}$	unit normal vector
P_0	atmospheric pressure
Q	heat effect
r	radial coordinate and position
R	reactor radius
$\mathbf{R}^2$	2D cylindrical metric space with axial symmetry
R_g	universal gas constant
S	condensed fuel mixture
S_{ex}	specific external reaction surface area
T	temperature
t	time
T_0	temperature of environment
T_A	heat-pulse amplitude
t_A	heat-pulse duration
T_b	maximal temperature in front of a wave
t_C	time in investigated system

u	velocity of solid fuel motion through the reactor
$\mathbf{U}$	vector unknowns
v_g	gas velocity
w	velocity of combustion front propagation
W	rate of a chemical reaction
Y	molar fraction of species in a gas
z	axial coordinate and position
Z	length of reactor
α_{out}	ratio of molar share of oxygen in gaseous products of burning/Y_{O2}^0
$\Delta H°$	change of standard enthalpy accompanying a reaction
θ	angular coordinate
λ	effective thermal conductivity of porous media
λ_0	thermal conductivity term
λ_σ	term of thermal conductivity by radiation
μ	stoichiometric coefficient
ρ	molar density in the medium
ρ_{g0}	density of gas at normal condition
Ω	two-dimensional domain, subset of $\mathbf{R}^2$

SUBSCRIPTS

0	initial or inlet value
i	index for gaseous active species
j	index for condensed active species
k	chemical reaction no.
K	number of chemical reaction
g	gas
I	inert solid material
C	solid carbon
O_2	oxygen
CO	carbon monoxide
CO_2	carbon dioxide
$MeCO_3$	carbonate
MeO	metal oxide
$MgCO_3$	magnesium carbonate
MgO	magnesium oxide
$CaCO_3$	calcium carbonate
CaO	calcium oxide
var	unknowns
gsp	gaseous active species
csp	condensed active species
N	number

INTRODUCTION

Co-flow filtration combustion of carbon is used in various large-scale industrial processes, such as coal gasification, roasting and sintering of ores, and direct reduction of iron from beneficiated iron ores. The process involves

---

[1]Current affiliation: Parker CRC for Integrated Hydrometallurgy Solutions, CSIRO Minerals, Bentley WA 6982, AUSTRALIA

combustion of a carbon-containing fuel in porous media with injected oxygen as an oxidising agent. When ignition occurs at the inlet, the reaction-combustion front travels in the direction of the injected gas leading to a co-flow filtration combustion (FC) or forward FC process (see Figure 1). The process of smoking a cigarette, for instance, represents an example of the co-flow filtration combustion.
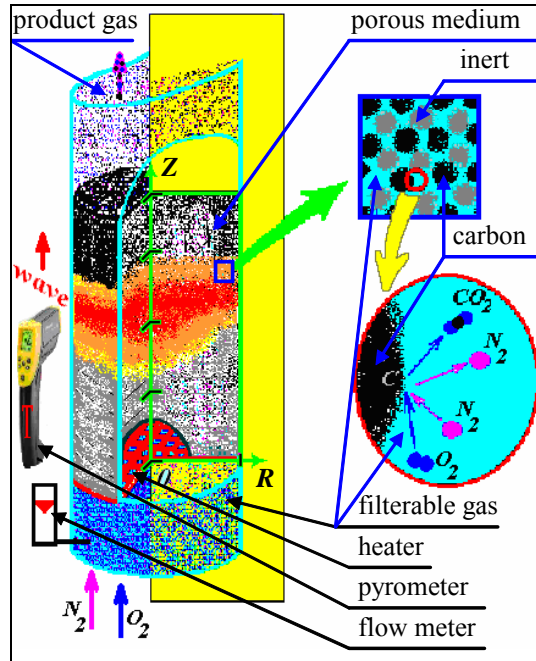
Figure 1. Schematic of the experimental setup for co-flow filtration combustion of carbon.

The co-flow FC process has been widely adopted by the industry due to its high economic efficiency (Aldushin et al., 1999), low environmental impact (Bingue et al., 2002), and technical simplicity. But in order to maintain its competitiveness, some of the limitations for the co-flow FC, such as instability of combustion front propagation, have to be unlocked. Two main types of instabilities exist: (i) dynamical instability of combustion front velocity (Shkadinskii et al., 1971) and (ii) spatially-temporal instabilities when combustion front changes shape (Lu & Yortsos, 2005). Filtration combustion systems can exhibit bifurcation behaviour (Vol'pert et al., 1984 and Weber et al., 2000) and structural reconstruction of these unstable regimes can be soft, hard and "chaotic" (Arn'old et al., 1994, and Nekhamkina & Sheintuch, 2002).

This work focuses mainly on studying the influence of complex interactions between chemical reaction kinetics on the stability of front propagation in the co-flow filtration combustion wave. A 2-D dynamic process model, developed in this work, describes the behavior of a cylindrical filtration-combustion reactor of a finite length. Axial symmetry was applied in order to reduce the size of the resulting numerical problem. The numerical model, which is based on mass and energy balance equations, incorporates relevant thermodynamic and kinetic laws to describe chemical transformations in solid and gaseous phases. The developed model is used to explore the effect of the mixture of filtering gas on the propagation of the heterogeneous combustion front through porous media,

i.e. time evolutions of temperature and concentration distributions in the reactor. Concentration distributions of a number of components, such as carbon, solid inert material, O_2, CO, CO_2, and inert gas, are described in this non-adiabatic model. In the model, the coefficient of thermal conductivity of porous media was assumed to be a non-linear function of temperature. Heat losses to the environment were incorporated into the model via appropriate boundary conditions. Based on the numerical experiment, the existence of non-unique stationary regimes of filtration combustion is demonstrated for systems more complex than the one described by Becker & Polianczyk (2004).

STATEMENT OF THE PROBLEM

Nonuniqueness of stationary regimes of the propagation of combustion waves in gas-free condensed media was studied previously by other authors (Khaikin & Khudyaev, 1979; Kholopov & Khudyaev, 1998). Typically, they considered the wave with two parallel exothermal reactions ($S_1 \leftarrow S_0 \rightarrow S_2$), for which the initial condensed inflammable mixture, S_0, is the same. As demonstrated by Merzhanov & Khaikin (1992), such a wave can be both fast and slow, with jumps from one branch to another accompanied by a hysteresis. Discussions on steady wave regimes and conditions leading to the transition from one regime to another can be found in the papers quoted above. A review of the literature on multiplicity of the combustion wave regimes in the solid gas-free phase is given by (Kholopov & Khudyaev, 1998). In the same work, the non-unique steady regimes of combustion in the mixture of gases, with two competing reactions, is also discussed.

The system presented in this contribution (see also Becker & Polianczyk, 2004) is different from previously mentioned work, as it considers heterogeneous systems, in which active gaseous reagent Y_0 filters through the condensed combustible fuel mixture, S_0, and reacts with it via reversible reactions leading to two gas products ($Y_1 \leftrightarrow S_0 + Y_0 \leftrightarrow Y_2$). It is known that the choice of operating parameters, such as gas flow, proportion of the oxidiser, mass ratio between active and inert material, enables regulation of temperature in the combustion front. The temperature at the combustion front also determines which chemical reactions are predominant (Becker et al., 2004).

The non-uniqueness of combustion regimes considered in (Khaikin & Khudyaev, 1979 and Becker & Polianczyk, 2004) resulted from the temperature and concentration dependence of the rates of chemical reactions and also due to various thermal effects of different reactions present. In the case of co-flow FC systems, discussed in the present work and (Becker & Polianczyk, 2004), the temperature at the co-flow combustion front can be reached not only due to various thermal effects of different reactions, but also as a result of the regulation of processes of filtration cooling and superadiabatic heating.

Experimental verification of the operation of co-flow filtration combustion of carbon in more than one stationary mode would be of great practical interest. However, the domain of operational conditions, where non-unique regimes in filtration combustion are expected, is quite narrow (Becker & Polianczyk, 2004). This makes

experimental verification of nonuniqueness a challenging problem, as different stationary regimes may be quite sensitive to the temperature drop resulting from heat losses to the environment.

In the present work, a mathematical model is developed for heterogeneous systems, such as roasting of magnesium carbonate and calcium carbonate in *air* atmosphere. For these two systems, experimental validation of the non-uniqueness of stationary regimes of filtration combustion is expected to be much simpler than the one in (Becker & Polianczyk, 2004), where diluted oxygen (less than 3%) was used. Different from Becker & Polianczyk (2004), the influence of external heat losses on non-unique regimes of filtration combustion in these systems is addressed in this work. For this purpose a non-adiabatic 2-D model of co-flow filtration combustion of carbon is developed.

A 2-D MODEL OF CO-FLOW FILTRATION COMBUSTION OF CARBON

In developing a dynamic co-flow carbon filtration combustion model, we make use of a continuous model of forward FC from previous work Becker et al. (2004). Here, the existing mass and energy balance-based dynamic model is extended to 2-D to describe the behavior of a cylindrical filtration-combustion reactor of finite length. Due to the assumed cylindrical geometry, the model equations are transformed using cylindrical coordinates r, z, and θ. Furthermore, axial symmetry is applied to reduce the size of the resulting numerical problem. Due to the symmetry, the model solution is independent of θ, so the transformed equations are:

$$
\begin{cases}
\Omega = \{(r,z); r \in (0,R), z \in (0,Z)\} \subset \mathbf{R}^2 \ \ t \in (0, t_C] \\
(c_I \rho_I + \sum_j c_j \rho_j)(\dfrac{\partial T}{\partial t} - u\dfrac{\partial T}{\partial z}) + c_g G_0 \dfrac{\partial T}{\partial z} = \\
\qquad = \dfrac{1}{r}\dfrac{\partial}{\partial r}\left(r\lambda\dfrac{\partial T}{\partial r}\right) + \dfrac{\partial}{\partial z}\left(\lambda\dfrac{\partial T}{\partial z}\right) + \sum_k W_k Q_k, \\
\lambda = \lambda_0 + \lambda_\sigma T^3, \ \ G_0 = \rho_g v_g = const, \ P_0 = const, \\
m\dfrac{P_0}{R_g T}\dfrac{\partial Y_i}{\partial t} + G_0\dfrac{\partial Y_i}{\partial z} = \\
\qquad = m\rho_{g0} D\left(\dfrac{1}{r}\dfrac{\partial}{\partial r}\left(r\dfrac{\partial Y_i}{\partial r}\right) + \dfrac{\partial^2 Y_i}{\partial z^2}\right) + \sum_k \mu_{i,k} W_k, \\
\dfrac{\partial \rho_j}{\partial t} - u\dfrac{\partial \rho_j}{\partial z} = \sum_k \mu_{j,k} W_k, \qquad \rho_{g0} D = const, \\
i = 1...N_{gsp}, \qquad j = 1...N_{csp}, \qquad k = 1...K.
\end{cases} \quad (1)
$$

In Eq. 1, the total number of variables is $N_{var} = 1 + N_{gsp} + N_{csp}$. The unknowns T, $Y_1, \ldots, Y_{N\,gsp}$, and $\rho_1, \ldots, \rho_{N\,csp}$, represent the temperature in the system, mole fractions of gaseous phase and density of condensed active species, respectively. The set of governing PDEs in Eq. 1 defines the mathematical model for a general case of unsteady 2-D filtration combustion of condensed fuel diluted by inert component in the flow of active gas components. Darcy's law is not included in this system due to: (i) high concentration of inert solids, and (ii) high porosity indicated by a negligible pressure drop. High dilution of solid fuel by inert component results in

negligible changes of bulk material porosity during the gasification.

For Eq. (1), at $t \in [0, t_C]$ in rectangular $(0,0; R,Z)$, see Fig. 1., Neumann boundary condition ($\nabla \mathbf{U} \cdot \mathbf{n} \equiv \partial \mathbf{U}/\partial n = 0$), is valid. Here, $\mathbf{U}$ is the vector of unknowns and $\mathbf{n}$ is normal vector to Ω. In addition, others boundary conditions exist

$$
\begin{cases}
line\ 0,0-R,0: \ \ T = T_0 + T_A(t), \ Y_i = Y_i^{\ 0}, \ i = 1...N_{gsp}, \\
line\ R,0-R,Z: \ \lambda\dfrac{\partial T}{\partial r} = h\cdot(T - T_0); \\
line\ 0,Z-R,Z: \ \rho_j = \rho_j^{\ 0}, \ j = 1...N_{csp}, \ \text{if}\ u > 0.
\end{cases} \quad (2)
$$

The centre axis of the cylinder, $r = 0$, is not a boundary in the original problem, but in our 2-D treatment it has become one. We must give the artificial Neumann boundary conditions here for axial symmetrical statement of the problem. For the outer boundary the term $h\cdot(T-T_0)$ is a model of transversal heat transfer from external cylinder surface to the surroundings by convection.

The initial value for $\mathbf{U}(\Omega,t)$ at $\Omega = \{r \in [0,R], z \in [0,Z]\}$ is:

$$\mathbf{U}(\Omega,0) = [T_0, Y_1^{\ 0}, \ldots, Y_{Ngsp}^{\ 0}, \rho_1^{\ 0}, \ldots, \rho_{N\,csp}^{\ 0}]^T \quad (3)$$

N	Reaction	E_k, kJ/mol	$k_{0\,k}$, mol/(m²s)	ΔH°_{298}, kJ/mol
1	$C + O_2 \rightarrow CO_2$	74.0	9.2	-393.5
2	$C + \frac{1}{2}O_2 \rightarrow CO$	179.0	$37 \cdot 10^3$	-110.5
3	$C + CO_2 \rightarrow 2CO$	215.5	$18 \cdot 10^7$	172.5
4	$C + 2CO \rightarrow 2C + CO_2$	43.0	0.145	-172.5
5	$MgCO_3 \rightarrow MgO + CO_2$	160.0	$26 \cdot 10^7$	116.6
6	$MgO + CO_2 \rightarrow MgCO_3$	43.4	0.188	-116.6
7	$CaCO_3 \rightarrow CaO + CO_2$	200.0	$50 \cdot 10^3$	178.5
8	$CaO + CO_2 \rightarrow CaCO_3$	21.5	$25 \cdot 10^{-5}$	-178.5

Table 1: Kinetic and thermodynamic parameters for the reaction rates in Eq. 4 have been determined in the studies of Barin et al. (1977), Kohlmann et al. (2002), Han & Sohn (2002) and Becker et al. (2004).

The model in Eq. 1, based on mass and energy balance equations, requires relevant thermodynamic and kinetic laws to describe chemical transformations in the solid and gaseous phase. These constitutive equations reflect specific behaviour of the mixture of carbon and magnesium (or calcium) carbonate in the filtration combustion regime. A set of chemical reactions that correspond to the reaction rate model in Eq. 4 is presented in Table 1. Following from these, the number of gaseous active species (O_2, CO_2, and CO) N_{GSP} is 3, and the number of condensed active species (C, $MgCO_3$, MgO) N_{CSP} is also 3. The vector of unknowns is $\mathbf{U} = [T, Y_{O2}, Y_{CO2}, Y_{CO}, \rho_C, \rho_{MgCO3}, \rho_{MgO}]^T$.

$$
\begin{cases}
W_1 = k_1 \rho_C Y_{O_2} \exp(\dfrac{-E_1}{RT}), \ \ W_2 = k_2 \rho_C Y_{O_2}^{\ 1/2} \exp(\dfrac{-E_2}{RT}), \\
W_3 = k_3 \rho_C Y_{CO_2} \exp(\dfrac{-E_3}{RT}), \ W_4 = k_4 \rho_C Y_{CO}^{\ 2} \exp(\dfrac{-E_4}{RT}), \\
W_5 = k_5 \rho_{MgCO_3} \exp(\dfrac{-E_5}{RT}), W_6 = k_6 \rho_{MgO} Y_{CO_2} \exp(\dfrac{-E_6}{RT}), \\
W_7 = k_7 \rho_{CaCO_3} \exp(\dfrac{-E_7}{RT}), W_8 = k_8 \rho_{CaO} Y_{CO_2} \exp(\dfrac{-E_8}{RT}).
\end{cases} \quad (4)
$$

The set of equations for chemical reaction rates can be written in Arrhenius's form for the case of gasification of a mixture of carbon and magnesium (calcium) carbonate in a mixed air, CO, CO_2 atmosphere, as stated in Eq. 4.

Using the developed mathematical model the formation and propagation of the reaction front for solid fuel gasification in the filtration mode and the structure and stability of the front can be analysed. Note, that the model also describes the reversible reactions and the cooling effect at the combustion front due to the gasification of magnesium (calcium) carbonate. In the case of $u \neq 0$ the model describes a solid fuel motion through the reactor, whereas for $u = 0$ it describes the evolution of the combustion reaction front in a stationary bed of solids.

ANALYSIS OF COMBUSTION REGIMES FOR MAGNESIUM AND CALCIUM CARBONATE ROASTING

Analysis of stationary combustion regimes is based on the analytical method introduced in (Becker & Polianczyk, 2004), which was carried out using a 1-D version of the combustion filtration model, similar to the one outlined in Eqs.1-4. In our case, however, endothermic reactions of carbonate decomposition (such as $MeCO_3 \rightarrow MeO + CO_2$) are taken into account in addition to the development of (Becker & Polianczyk, 2004).
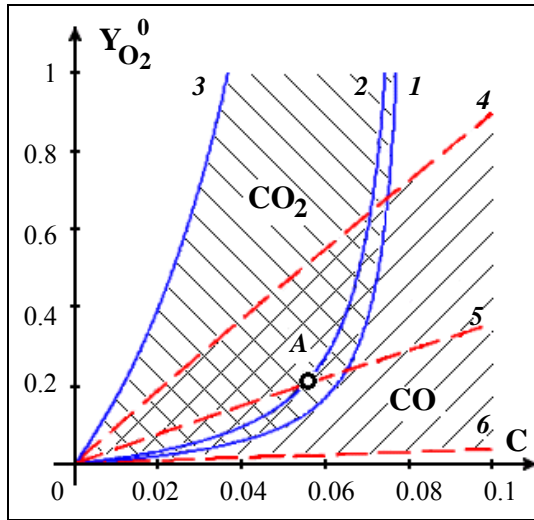
Figure 2. Lines of constant combustion temperature (T_b) for the MgCO3:C:SiO2 mixture in Y_{O2}^0 and C coordinates. Y_{O2}^0 – a molar share of oxygen in oxygen/nitrogen oxidant inlet gas: $C = \rho_C^0/\rho_{SiO2}$ – a molar ratio of carbon/silica in solid fuel. Line 1: T_b=850 K, α_{out} = 0; Line 2: T_b=850 K, α_{out} = 0.38; Line 3: T_b=850 K, α_{out} = 0.95. Dotted line 4: T_b=1500 K, α_{out} = 0.98; Dotted line 5: T_b=1500 K, α_{out} = 0.9; Dotted line 6: T_b=1500 K, α_{out} = 0.

Presented in Figures 2 and 3, are results that show necessary conditions (domains of operating parameters for air gasification of three-component systems, C:MgCO3:SiO2 and C:CaCO3:SiO2), at which co-flow filtration combustion of carbon in two different stationary regimes is possible. In this analysis, heat losses to the environment were assumed negligible. The domain CO_2, in between the lines 1 and 3 in Figure 2 and Figure 3 corresponds to low-temperature regimes with normal wave structure and residual oxygen fraction within (0,

0.95). The domain CO, in between the lines 4 and 6 in the same figures corresponds to high-temperature regimes with normal wave structure and residual oxygen fraction within (0, 0.98). In Figure 2, point A denotes the case of the air gas calcination of the mixture $MgCO_3$:C:SiO_2, where $\rho_{MgCO3}/\rho_C = 0.5$ is the ratio of molar density of magnesium carbonate and carbon in the solid fuel. In Figure 3, point B denotes the case of the air gas calcinations of the mixture $CaCO_3$:C:SiO_2, where $\rho_{CaCO3}/\rho_C = 0.4$ is the ratio of molar density of calcium carbonate and carbon in the solid fuel.
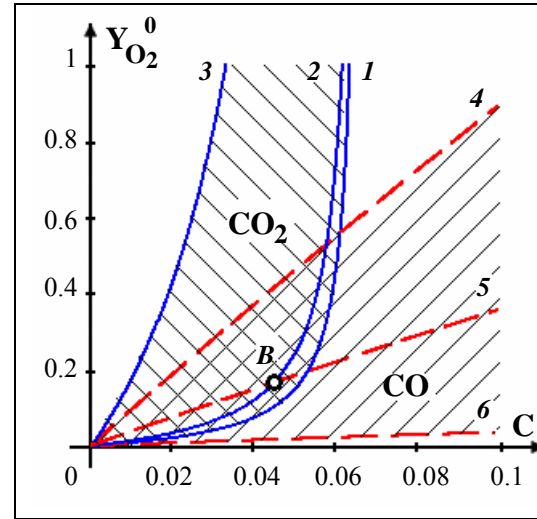
Figure 3. Lines of constant combustion temperature (T_b) for the CaCO3:C:SiO2 mixture in Y_{O2}^0 and C coordinates. Line 1: T_b=850 K, α_{out} = 0; Line 2: T_b=850 K, α_{out} = 0.38; Line 3: T_b=850 K, α_{out} = 0.95; Dotted line 4: T_b=1500 K, α_{out} = 0.96; Dotted line 5: T_b=1500 K, α_{out} = 0.9; Dotted line 6: T_b=1500 K, α_{out} = 0.

Parametric domains that include points A, B represent the intersection of CO_2 and CO lines at the point of Y_{O2}^0 and C, where non-unique solution regimes may be expected. Within this domain a normal wave structure with T_b=850 K and normal wave structure with T_b=1500 K can exist for the same operational parameters. This shows that non-unique stationary regimes are possible in more complex filtration combustion systems than the carbon filtration combustion (Becker & Polianczyk, 2004).

NUMERICAL RESULTS

The case of air gasification of the mixture of carbon, silica (inert), and magnesium carbonate in filtration combustion regime, which takes into account chemical reactions 1-6 in Table 1, was investigated numerically by solving mathematical model (Eqs.1–4) for the following model parameter values: R=0.5 m; Z = 2 m; t_A = 1500 s; m = 0.5; ρ_C^0 = 1200 mol/m³; ρ_{MgCO3}^0 = 600 mol/m³; ρ_{MgO}^0 = 0 mol/m³; ρ_I = 23300 mol/m³; $c_{MgCO3}=c_{MgO}=c_C=c_I$ = 44 J/(mol·K); c_g = 33 J/(mol·K); P_0 = 10⁵ Pa; T_0 = 298 K; Y_{O2}^0 = 0.21; Y_{CO2}^0 = 0; Y_{CO}^0 = 0; Q_1 = 397 kJ/mol; Q_2 = 115 kJ/mol; Q_3 = − 184 kJ/mol; Q_4 = 184 kJ/mol; Q_5 = − 127 kJ/mol; Q_6 = 127 kJ/mol; k_1 = 3.3·10⁴ s⁻¹; k_2= 1.33·10⁸ s⁻¹; k_3 = 6.48·10¹¹ s⁻¹; k_4= 522 s⁻¹; k_5 = 4.37·10¹¹ s⁻¹; k_6 = 316 s⁻¹; E_1 = 74 kJ/mol; E_2 = 179 kJ/mol; E_3 = 215.5 kJ/mol; E_4 = 43 kJ/mol; E_5 = 160 kJ/mol; E_6 = 43.4 kJ/mol; G_0 = 3 mol/(m²·s) ; λ_0 = 0.5 W/(m·K); λ_σ = 2.4·10⁻⁹ W/(m·K⁴); $\rho_g D$ = 1.26·10⁻⁴ mol/(m·s); h=6.5 W/(m²·K);

u=0 (m/s). The above conditions were chosen such to reproduce the intersection point **A** of Figure 2.

The pre-exponential kinetic parameters were calculated as $k_k = k_{0k} \cdot S_{ex} \cdot M$ according to the data in *Table 1*. Note that M is the molar mass in g/mol. Specific surface area was S_{ex}=300 m²/g for carbon (activated charcoal) and S_{ex}=20 m²/g for magnesium carbonate and magnesium oxide. All thermodynamic parameters were estimated at T_b=800 K.

A fully implicit finite-element approximation of the set of nonlinear partial differential equations (Eqs.1–4) was iteratively solved at each time step using Newton's method and adaptive mesh strategy. Concentration distributions in the reactor of a number of active components, such as O_2, CO, CO_2, carbon, magnesium carbonate and magnesium oxide, were predicted.

Figure 4 and 5 shows <u>modelling results for an idustrial-scale batch superadiabatic calciner</u> with the 2D region initially being charcoal and magnesium carbonate particles. Air is injected into the base of the porous carbon-containing medium as shown by O_2 plot (see also Fig. 1). This reacts with the carbon particles producing carbon dioxide and carbon monoxide gases and heat for carbonate roasting. Other plots show the concentration of these species and distribution of the temperature and gas velocity within the superadiabatic calciner.

In the Figure 4 and 5, operational maps are presented as resulted from two computational experiments. The distributions, presented in both figures illustrate normalised values of the respective variables in the range from *min* to *max* value.
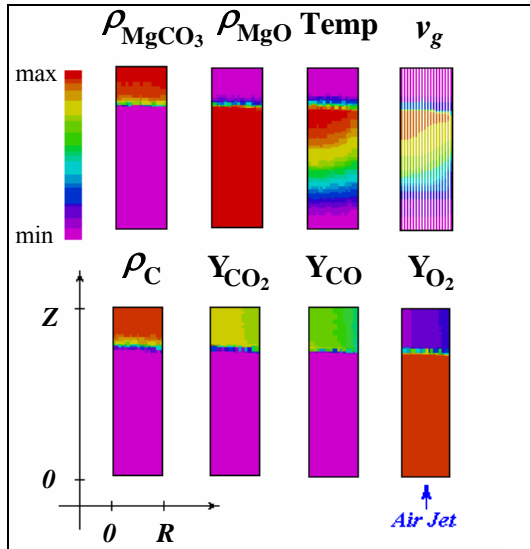
Figure 4. Temperature, gas velocity and concentration distributions in the reactor at t_C = 8100 s. Temp (298 K, 850 K); v_g (0.07 m/s, 0.20 m/s); Y_{O2} (0.13, 0.21); Y_{CO2} (0, 0.20); Y_{CO} (0, 0.03); ρ_C (0 mol/m³, 1200 mol/m³); ρ_{MgCO3} (0 mol/m³, 600 mol/m³); ρ_{MgO} (0 mol/m³, 600 mol/m³).

Shown in Figure 4, are the results from the first numerical experiment, where ignition pulse, T_A, of 502 K was applied in the numerical simulation. In this *low-temperature regime*, the operation results in a combustion wave with a distinct *normal structure,* where high temperature region follows behind the reaction front, as indicated in the temperature map in Figure 4. Combustion products, in this case, consist predominantly of carbon dioxide (ratio [CO]/[CO₂] below 0.03). Note that the resulting low-temperature regime, simulated in this computational experiment, is non-stoichiometric. Residual oxygen, around 38% of the amount in the inlet, is present in combustion products. The established combustion temperature agrees well with the value obtained by the 1-D analysis of similar combustion regimes (Becker & Polianczyk, 2004).
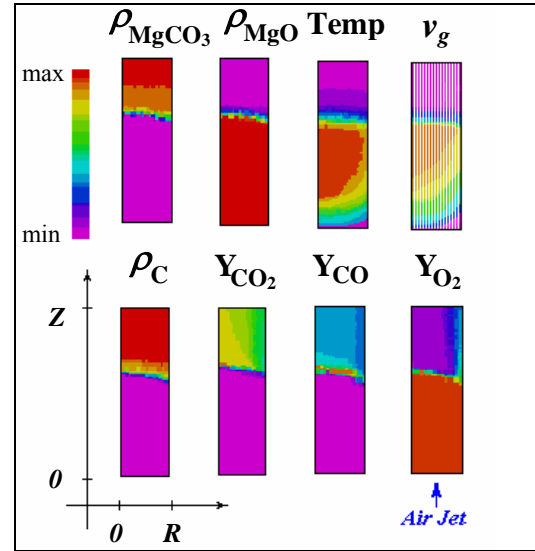
Figure 5. Temperature, gas velocity and concentration distribution in the reactor at t_C = 9500 s. Temp (298 K, 1450 K); v_g (0.07 m/s, 0.4 m/s); Y_{O2} (0.18, 0.21); Y_{CO2} (0, 0.04); Y_{CO} (0, 0.20); ρ_C (0 mol/m³, 1200 mol/m³); ρ_{MgCO3} (0 mol/m³, 600 mol/m³); ρ_{MgO} (0 mol/m³, 600 mol/m³).

In the second numerical experiment, shown in Figure 5, the case with the ignition pulse, T_A, of 1202 K resulted in a very different *high-temperature combustion regime*. The combustion zone, in this case, attained a much higher temperature. Similar to the first case, the combustion wave also exhibited a *normal wave structure*, and high temperature zone was present behind the reaction front. The only combustion product in this high-temperature case is carbon monoxide ([CO₂]/[CO] < 0.05). This case operates under a strong *kinetic regime*, with only 10% of inlet oxygen consumed in the reaction. Effects, which influence the amount of CO, include the inhibition of gaseous reaction CO+½O₂→CO₂, and quenching of the product gas in the combustion wave with normal structure. As a result CO emerges as the dominant combustion product in a *high-temperature combustion regime*, even when excess oxygen is present. This phenomenon has been discussed from thermodynamic and kinetic point of view by Becker *et al.* (2004).

In both regimes, low and high temperature one, the fraction of un-reacted carbon is very low, less than 0.001%. Velocities of combustion front propagation for the two regimes are different. For the low-temperature regime the velocity is 2.0·10⁻⁴ m/s, whereas for high-temperature regime it is 1.5·10⁻⁴ m/s.

For both regimes the magnesium carbonate was fully converted to magnesium oxide. This confirms that the magnesium carbonate conversion can be approximated by a single reaction pathway, $MgCO_3 \rightarrow MgO + CO_2$.

In the case of an *inverse structure* wave*,* where high temperature region travels ahead of the combustion front (Becker & Polianczyk, 2004) stationary combustion regimes do not exist for the system $C:MeCO_3:SiO_2$ because carbonates decomposition takes place on the forward border of the warming front, which escapes from the combustion front.

CONCLUSIONS

The process of co-flow filtration combustion of carbon-containing materials in superadiabatic regimes was studied numerically with the aid of a 2-D dynamic model.

A reduced dimensionality model (1-D) was used in analytical investigation of the behaviour of the co-flow combustion process. Based on this analysis, new physical phenomenon in the form of non-unique stationary regimes of filtration combustion of carbon was demonstrated. The occurrence of multiple combustion regimes is a consequence of the fact that oxidation of carbon can lead to two different oxides, with a further, thermodynamically reversible, transition possible between them.

2-D simulation results show that under similar process conditions the oxidation of carbon in co-flow filtration combustion can lead to two different operating regimes of the combustion wave propagation. In a higher temperature regime, a higher fraction of CO develops at the combustion wave-front. In the regime at lower temperature, CO_2 is the predominant gas product at the reaction front. The temperature at the reaction front for the two regimes differs not only due to different enthalpy effects in the generation of CO and CO_2, but mainly due to its self-congruent regulation in the filtration cooling and superadiabatic heating regimes. Operations at different non-unique modes result in radical changes in temperature, wave velocity, and composition of combustion products. It was shown that for the systems such as magnesium or calcium carbonate roasting, a range of operation parameters exist, for which more than one stationary filtration combustion regime is possible.

In the *normal structure* wave of filtration combustion, where high temperature region follows behind the combustion front, metal carbonates decay directly in the combustion front. In the *inverse structure* wave*,* where high temperature region travels ahead of the combustion front, for a system (carbon:$MeCO_3$:solid inert*)* stationary regimes of filtration combustion do not exist because decomposition of the metal carbonate originates on a forward border of warming front, which escapes from the combustion front.

REFERENCES

ALDUSHIN A.P., RUMANOV I.E., MATKOWSKY B.J., (1999), "Maximal energy accumulation in a superadiabatic filtration combustion wave", *Combustion and Flame*, **118-1**, 76-90.

ARN'OLD V. I., AFRAIMOVICH V., IL'YASHENKO Y., and SIL'NIKOV L., (1994), "Theory of bifurcations", Encyclopaedia of Mathematical Sciences, vol. 5, (V. I. Arn'old, ed.), *Springer-Verlag*, Berlin and New York.

BARIN I., KNACKE O. and KUBARSCHEWSKI O., (1977), "Thermochemical Properties of Inorganic Substances", *Springer-Verlag*, Berlin.

BECKER A.V. and POLIANCZYK E.V., (2004), "Non-unique stationary regimes of filtration combustion of carbon", *Proceedings of International Conference on Combustion and Detonation.* Zel'dovich Memorial II, Moscow, Russia, August 30-September 3, 8 pages.

BECKER A.V., POLIANCZYK E.V., VOLKOVA N. N. and MANELIS G. B., (2004), "Modeling of Filtration Combustion of Carbon", *Theoretical Foundations of Chemical Engineering*, **38-5**, 510-516.

BINGUE J.P., SAVELIEV A.V., FRIDMAN A.A. and KENNEDY L.A., (2002), "NOx and CO Emissions of Lean and Ultra-lean Filtration Combustion of Methane / Air Mixtures in an Inert Porous Media", *Clean Air*, **3**, 199 -210.

HAN D. H. and SOHN H. Y. (2002), "Calcined Calcium Magnesium Acetate as a Superior SO Sorbent: I. Thermal Decomposition", *AIChE Journal.*, **48-12**, 2971-2977.

KHAIKIN B.I. and KHUDYAEV S.I., (1979), "Nonuniqueness of combustion temperature and rate when competing reactions take place", *Dokl. Phys. Chem.*, **245**, 225-228.

KHOLOPOV V.M. and KHUDYAEV S.I., (1998), "Multiplicity of steady combustion wave", *Mathematical modelling*. (Russian) **10-5**, 91-108.

KOHLMANN J., ZEVENHOVEN R. and MUKHERJEE A.B., (2002), "Carbon Dioxide Emission Control by Mineral Carbonation: The Option for Finland", *INFUB 6th European Conference on Industrial Furnaces and Boilers,* Estoril Lisbon, Portugal, April 2-5, 10 pages.

LU C. AND YORTSOS Y. C., (2005), "Dynamics of forward filtration combustion at the pore-network level" *AIChE Journal*, **51- 4,** 279-1296.

MERZHANOV A.G. and KHAIKIN B. I., (1992), "The Theory of Combustion Waves in Homogeneous Media", (Russian), *Chernogolovka: Institute of Structural Macrokinetics RAS.*

NEKHAMKINA O. and SHEINTUCH M., (2002), "Spatially "chaotic" solutions in reaction-convection models and their bifurcations to moving waves", *Phys. Rev. E*, **66**, 016204, 5 pages.

SHKADINSKII K.G., KHAIKIN B.I., and MERZHANOV A.G., (1971), "Propagation of a pulsating exothermic reaction front in the condensed phase", *Combustion, Explosion and Shock Waves*, **7-1**, 19-28.

VOL'PERT V. A., VOL'PERT A. I. and MERZHANOV A. G., (1984), "Application of the theory of bifurcations to the investigation of nonstationary combustion regimes", *Combustion, Explosion, and Shock Waves,* **19-4**, 435-438.

WEBER R.O., MERCER G.N. and SIDHU H.S., (2000), "Bifurcating combustion behaviour", *ANZIAM J.* **42-E**, 1465-1481.